Available online at www.sciencedirect.com
ScienceDirect
Journal of Sound and Vibration 314 (2008) 83–94
JOURNAL OF SOUND AND VIBRATION
www.elsevier.com/locate/jsvi

Vibration and damage detection in undamaged and cracked circular arches: Experimental and analytical results

M.N. Cerri[a,1], M. Dilena[b], G.C. Ruta[c,*]

[a]Istituto di Scienza e Tecnica delle Costruzioni, Università Politecnica delle Marche, Ancona, Italy
[b]Dipartimento di Georisorse e Territorio, Università di Udine, Udine, Italy
[c]Dipartimento di Ingegneria Strutturale e Geotecnica, Università "La Sapienza", Via Eudossiana 18, 00184 Rome, Italy

Received 10 July 2007; received in revised form 22 December 2007; accepted 7 January 2008
Handling Editor: C. Morfey
Available online 7 March 2008

Abstract

This paper presents the experimental results of the dynamic behaviour of a circular arch in undamaged and several damaged configurations, and compares them with those obtained by means of analytical methods. The damage is introduced in the undamaged arch by operating a notch and is then modelled as a torsion spring of suitable stiffness localised in the damaged cross-section. Good agreement between analytical and experimental results is observed. An identification procedure based on frequency measurements is proposed and validated.

1. Introduction

In recent years there has been a growing interest towards non-destructive techniques of structural monitoring, for instance by means of dynamic quantities [1–5]. This paper follows the same field of research and is intended to show the measured modal quantities in a plane circular arch. Dynamic tests are performed first for the undamaged arch, and then in the same arch damaged by means of a localised notch. The experimental results are here compared with the same quantities as obtained by an analytical model.

The specimen considered for the experiments consists of a circular arch made of steel with a thin (compared with the arch span) rectangular section, hinged at both ends (Fig. 1). Measurements are performed at least for the first five natural frequencies and the radial components of the first four natural vibration modes of the specimen. The experimental tests are performed on the undamaged arch, then are repeated on the same arch after having caused a damage on it. The damage consists in a very thin notch, which could then be thought as localised in a narrow neighbourhood of the considered cross-section; the depth of the notch is progressively increased until half of the height of the section is reached.

*Corresponding author. Tel.: +39 06 44585085; fax: +39 06 4884852.
E-mail addresses: m.n.cerri@univpm.it (M.N. Cerri), michele_dilena@email.it (M. Dilena), giuseppe.ruta@uniroma1.it (G.C. Ruta).
[1]Maria Nilde Cerri passed away on June 24, 2005, at the age of 42. This paper is intended to be a testimonial of affection to a much beloved colleague and, most of all, friend. M.D. and G.C.R.

0022-460X/$ - see front matter © 2008 Elsevier Ltd. All rights reserved.
doi:10.1016/j.jsv.2008.01.029

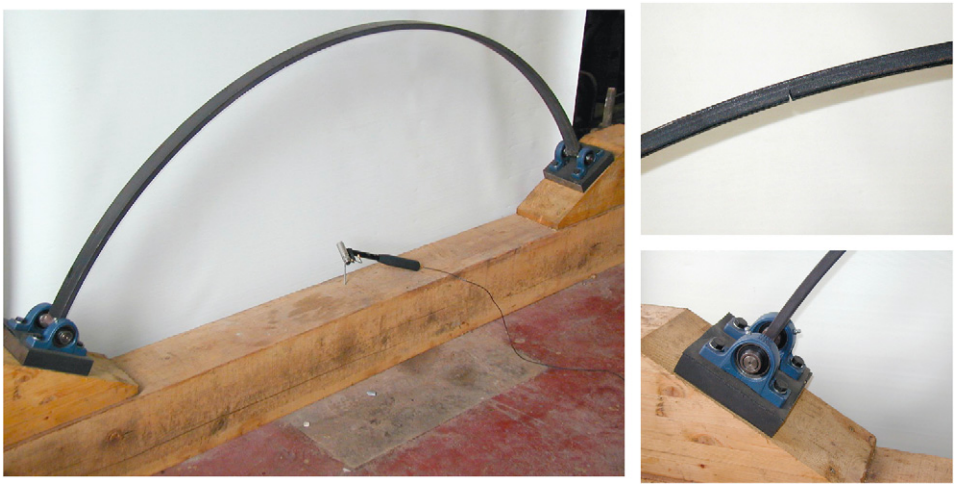

Fig. 1. Circular arch specimen: particulars of the notch and of the hinged end.

The experiments show that the variation of the natural frequencies between the undamaged and the damaged configurations are small, but in any case appreciable. On the other hand, the natural vibration modes reveal themselves as almost insensitive to these localised damage levels.

In order to have analytical results to compare with the measured experimental ones, a direct one-dimensional (1D) model is used. In a previous paper [6], some of the authors examined different models, by successively neglecting the shearing strain between the cross-sections and the axis, the rotary inertia, the extension of the axis and the tangential inertia. In this paper, though, since we deal with experimental measurements, a 1D arch model with no inner constraints is adopted.

The damage is considered as a singularity in the bending stiffness of the arch, and thus is modelled as a torsion spring with a suitable stiffness, localised in the section where the damage is caused.

The obtained experimental results are in good agreement with the analytical estimates. In the case of the natural frequencies, the differences between the values given by the analytical model and the measured ones increase with the mode order; in any case, the errors are less than 4%. As far as the vibration modes are concerned, a very good correspondence is observed. A diagnostic technique based on the frequency sensitivity to damage is also applied and allows a rather precise identification in all the configurations studied in the experiments.

2. Direct problem

2.1. Analytical model

In order to model homogeneous circular arches, both in the undamaged and in the damaged configuration, analytical models already present in the literature are taken into account, some examples of which are given in Refs. [6–14].

Let us consider a circular arch in undamaged configuration hinged at both ends (Fig. 2a); moreover, let us suppose that the arch undergoes free linear vibration in its own plane. Due to the supposed linearity, the oscillations are "small" and limited to a neighbourhood of the reference configuration, which is the one depicted in Fig. 2a.

Kinematics of the arch are described by means of the displacement components of the axis in the tangential and radial direction, denoted by u and v, respectively, and by means of the cross-section rotation, denoted by φ. All the kinematical fields are supposed to be regular enough functions of the angular abscissa $\theta \in [-\Theta,\Theta]$ along the arch axis and of the time t. The chosen kinematics is the richest as possible for a 1D continuum, in order to match, at least in principle, with experimental outcomes.

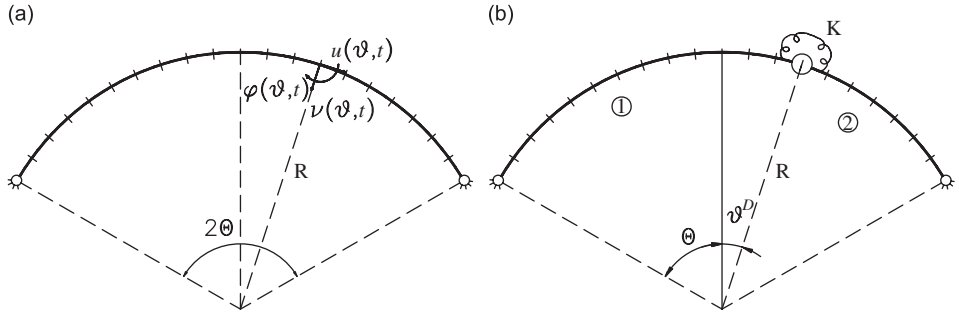

Fig. 2. Geometry of the arch: (a) in the undamaged and (b) damaged configuration.

The scalar equations of the free motion are [8–11]

$$\begin{aligned}
&\frac{EA}{R^2}\frac{\partial}{\partial\theta}\left(\frac{\partial u(\theta,t)}{\partial\theta}-v(\theta,t)\right)-\frac{GA}{R^2\chi}\left(u(\theta,t)+\frac{\partial v(\theta,t)}{\partial\theta}+R\varphi(\theta,t)\right)=\rho A\frac{\partial^2 u(\theta,t)}{\partial t^2},\\
&\frac{GA}{R^2\chi}\frac{\partial}{\partial\theta}\left(u(\theta,t)+\frac{\partial v(\theta,t)}{\partial\theta}+R\varphi(\theta,t)\right)+\frac{EA}{R^2}\left(\frac{\partial u(\theta,t)}{\partial\theta}-v(\theta,t)\right)=\rho A\frac{\partial^2 v(\theta,t)}{\partial t^2},\\
&\frac{EI}{R^2}\frac{\partial^2\varphi(\theta,t)}{\partial\theta^2}-\frac{GA}{R\chi}\left(u(\theta,t)+\frac{\partial v(\theta,t)}{\partial\theta}+R\varphi(\theta,t)\right)=\rho I\frac{\partial^2\varphi(\theta,t)}{\partial t^2},
\end{aligned}\tag{1}$$

supplemented by the boundary conditions

$$\begin{aligned}
&u(-\Theta,t)=u(\Theta,t)=0,\\
&v(-\Theta,t)=v(\Theta,t)=0, \qquad t>0.\\
&\frac{\partial\varphi(-\Theta,t)}{\partial\theta}=\frac{\partial\varphi(\Theta,t)}{\partial\theta}=0,
\end{aligned}\tag{2}$$

In Eq. (1), R is the radius of the circumference which the arch axis is part of, ρ is the mass density per unit volume of the material of the arch. A and I are the area and the relevant moment of inertia of the cross-section, respectively. E and G are the longitudinal and tangential moduli of elasticity, respectively, and χ is the shear shape factor of the cross-section.

As it is customary in free vibration, a harmonic solution with respect to time, of natural angular frequency ω, is looked for. In this way, a system of ordinary differential equations with respect to the variable θ is obtained, which may be solved by applying the technique of Euler's characteristic exponents, in order to obtain exact solutions of the problem of the free vibration of the arch (see Refs. [13,14]).

Suppose now that the arch is damaged by a notch located at the angular coordinate θ^D. This situation is modelled by dividing the arch into two continuous parts linked by means of a torsion spring of stiffness K located at θ^D, as shown in Fig. 2b. As suggested in a previous paper [6], the value of K can be approximated supposing that the actual damage is distributed in a narrow zone of amplitude $\Delta\theta^D$ and that the bending stiffness is constant in that zone. In analogy with the case of a rectilinear beam [7], it is possible to provide an estimate of the stiffness K according to the following expression:

$$K=\frac{EI^D}{(EI-EI^D)}\frac{EI}{\Delta\theta^D R},\tag{3}$$

where EI^D is the flexural stiffness in the neighbourhood of the notch and $\Delta\theta^D R=H/\alpha$, with H the height of the cross-section and α approximately equal to 2 (see also Ref. [15]). Then, the damaged arch consists of two regular undamaged parts, each governed by the system of Eqs. (1). In addition to the boundary conditions (2),

the following jump conditions hold at the damaged cross-section (see also Refs. [13–16]):

$$\begin{aligned} u^{(2)}(\theta^D,t)-u^{(1)}(\theta^D,t)&=0,\\ v^{(2)}(\theta^D,t)-v^{(1)}(\theta^D,t)&=0,\\ K(\varphi^{(2)}(\theta^D,t)-\varphi^{(1)}(\theta^D,t))&=M^{(1)}(\theta^D,t),\quad t>0,\\ N^{(2)}(\theta^D,t)-N^{(1)}(\theta^D,t)&=0,\\ V^{(2)}(\theta^D,t)-V^{(1)}(\theta^D,t)&=0,\\ M^{(2)}(\theta^D,t)-M^{(1)}(\theta^D,t)&=0, \end{aligned} \tag{4}$$

where the apexes (1) and (2) imply that the considered field refers to the left and the right undamaged parts of the arch, respectively. The inner actions N and V (i.e., the tangential and radial component of the force) and M (i.e., the unique bending component of the moment) are expressed in terms of the kinematical fields via the standard linear elastic constitutive relations

$$\begin{aligned} N(\theta,t)&=\frac{EA}{R}\left(\frac{\partial u(\theta,t)}{\partial\theta}-v(\theta,t)\right),\\ V(\theta,t)&=\frac{GA}{R\chi}\left(u(\theta,t)+\frac{\partial v(\theta,t)}{\partial\theta}+R\varphi(\theta,t)\right),\\ M(\theta,t)&=\frac{EI}{R}\frac{\partial\varphi(\theta,t)}{\partial\theta}. \end{aligned} \tag{5}$$

It is possible and not difficult to extend the solving procedure adopted in the undamaged case and hence provide exact solutions.

2.2. Experimental tests

The dynamical quantities measured on the specimen are the natural frequencies and the radial component of the displacement, i.e., of the natural vibration modes. The tests are performed four times: the first one is carried out on the undamaged arch, the others by introducing a notch of increasing depth: 2.5 mm (D1), 5.0 mm (D2) and 7.5 mm (D3). The notch is localised in a section placed at 16.5° with respect to the axis of symmetry of the arch (see particulars of Fig. 1). The specimen used in the tests is obtained by bending an initially straight element according to an arc of a circumference (Fig. 3).

The nominal geometric and material characteristic properties of the specimen are shown in Table 1. The arch is hinged to the ground by means of two hinges, which are made by rollers fixed on suitable supports (see particulars of Fig. 1).

The experimental activity is carried out at the laboratory of the Istituto di Scienza e Tecnica delle Costruzioni of the Università Politecnica delle Marche in Ancona, Italy. The tests are performed by using the

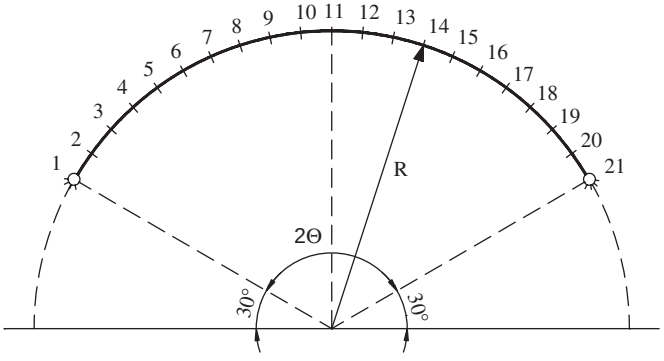

Fig. 3. Geometry of the experimental specimen.

Table 1
Nominal geometric and material characteristic properties of the steel arch specimen

Characteristic properties	Values
Young's modulus (of longitudinal elasticity), E	206,000 MPa
Shear modulus (of tangential elasticity), G	80,000 MPa
Mass density, ρ	7850 kg/m^3
Radius of the axis of the arch, R	1000 mm
Angular span of the arch, 2Θ	120°
Base of the cross-section, B	45 mm
Height of the cross-section, H	15 mm
Area of the cross-section, A	675 mm^2
Relevant moment of inertia of the cross-section, I	12,656 mm^4

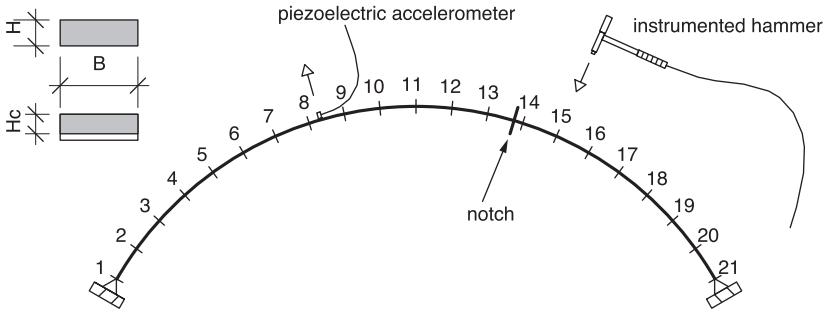

Fig. 4. Sketch of the experimental apparatus and of the measurement points.

impulsive technique, the main features of which are a high speed of execution and a good reproducibility of the measured quantities [17].

The arch is excited by means of a Brüel and Kjær hammer, type 8202, endowed with a tip rigid enough in the frequency range considered during the experiments. The acquisition of the dynamic response is obtained by means of a piezoelectric Brüel and Kjær accelerometer, type 4508. The input signal is processed by force windows with time amplitude equal to 1/10 of the recording time; the output signal is filtered by an exponential window with time decay constant $c = 1/4$. The signals are acquired and transferred in the frequency domain by means of a Brüel and Kjær signal analyser, working under a PULSE LabShop system.

The frequency response functions in terms of inertance are extracted from the data obtained by the acquisition system. After coarsely detecting the values of the natural frequencies, inertance is assessed in the neighbourhood of span 25 Hz, centred on each value of resonant frequency with a resolution of 1/16 Hz. Each frequency response function is evaluated as the average over 10 tests, because of the good reproducibility of the measurements. Since the values of the natural frequencies are far enough from each other, and the value of the damping is small, it is possible to make use of the single mode extracting technique. For each frequency response function, the values of the natural frequency, of the damping and of the modal residuals are extracted by means of a curve-fitting procedure based on a least-squares interpolation algorithm.

The arch is divided into 20 elements, each with an angular span of 6°; in this way, 21 measurement points are singled out (Fig. 4). For higher-order modes and in the undamaged case only, these measurement stations are doubled. The radial components of the first four natural vibration modes are determined by fixing the position of the accelerometer and by varying the point where the arch is excited, i.e., in correspondence with the considered measurement points. The magnitude of each frequency response function at the resonance value is proportional to the transversal component of displacement of the pertaining natural vibration mode.

2.3. Experimental results and comparisons

The first five natural frequencies for the undamaged and for the three damaged configurations of the arch are shown in Table 2. As expected, a progressive decrease in the value of the natural frequencies with respect to the increase in the depth of the notch is observed. The corresponding variations between the undamaged and damaged states are small, but clearly detectable starting from the first level of damage and not mistaken with measurements errors. As an example, the third vibrating mode is the most sensitive to the presence of the notch, with frequency variations equal to 0.25% and 1.37%, respectively, for D1 and D3 damage configuration. Conversely, the fourth mode is practically insensitive to the damage.

Fig. 5 shows the plots of the experimental results concerning the radial component of the displacement in the first four vibration modes for the undamaged and the D3-damaged arch. The behaviour of the radial component of the displacement shows a satisfactory regularity, both in the undamaged and in the damaged

Table 2
Experimental natural frequencies and their variation (in percentage) for different damage amounts

Mode	Undamaged	Damage D1		Damage D2		Damage D3	
	Frequency (Hz)	Frequency (Hz)	Variation (%)	Frequency (Hz)	Variation (%)	Frequency (Hz)	Variation (%)
1	24.52	24.48	0.18	24.40	0.48	24.32	0.80
2	61.78	61.72	0.10	61.66	0.20	61.60	0.30
3	118.05	117.76	0.25	117.11	0.80	116.43	1.37
4	184.11	184.03	0.04	183.91	0.11	183.81	0.16
5	269.02	268.24	0.29	268.43	0.22	267.94	0.40

Frequency variation: $\Delta f = 100(f_{und} - f_{dam})/f_{und}$.

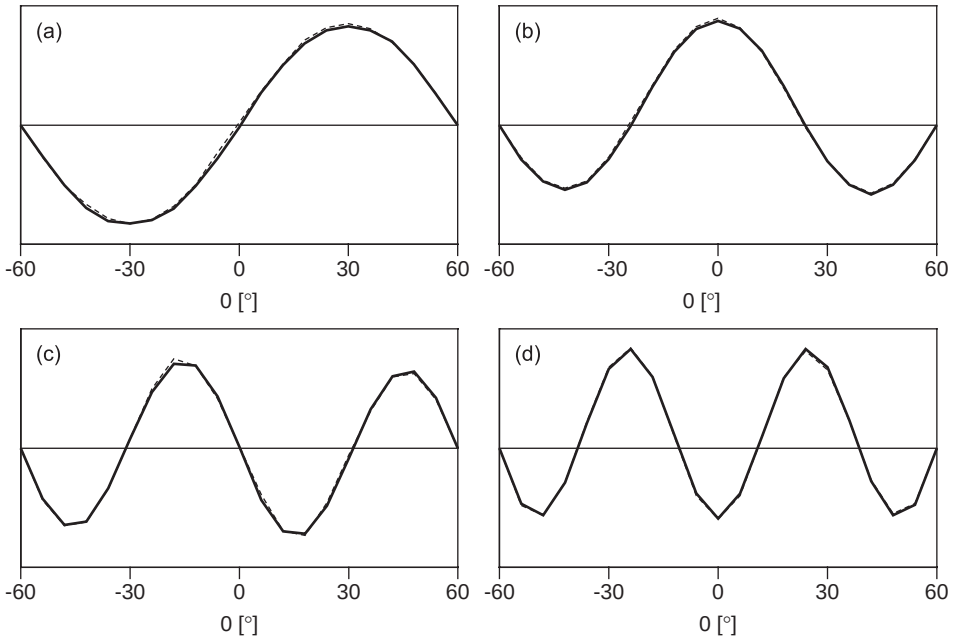

Fig. 5. Radial component of the first four mode shapes for the undamaged and the D3-damaged arch: (a) first mode, (b) second mode, (c) third mode, and (d) fourth mode. Undamaged configuration: solid thick line and damaged configuration: dashed thin line.

Table 3
Experimental and analytical natural frequencies for the considered arch specimen

Mode	Undamaged			Damage D1			Damage D2			Damage D3		
	E (Hz)	A (Hz)	Δ (%)	E (Hz)	A (Hz)	Δ (%)	E (Hz)	A (Hz)	Δ (%)	E (Hz)	A (Hz)	Δ (%)
1	24.52	24.62	0.4	24.48	24.61	0.6	24.40	24.54	0.6	24.32	24.29	−0.1
2	61.78	62.14	0.6	61.72	62.14	0.7	61.66	62.11	0.7	61.60	62.01	0.7
3	118.05	119.92	1.6	117.76	119.81	1.7	117.11	119.24	1.8	116.43	117.15	0.6
4	184.11	189.52	2.9	184.03	189.48	3.0	183.91	189.22	2.9	183.81	188.32	2.5
5	269.02	279.09	3.7	268.24	279.02	4.0	268.43	278.64	3.8	267.94	277.23	3.5

E: experimental; A: analytical; $\Delta = 100(f_{anal}-f_{exp})/f_{exp}$: error.

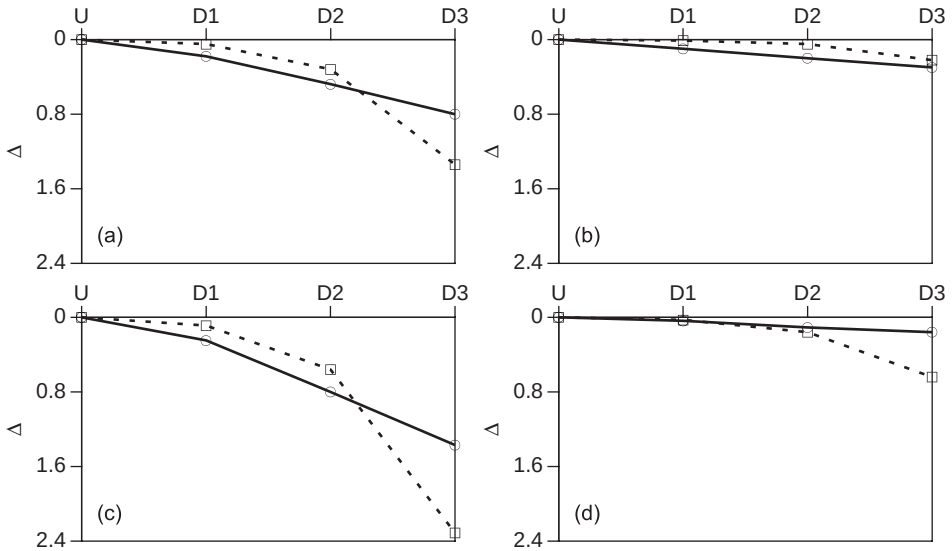

Fig. 6. Relative variation of natural frequencies vs. increasing damage severity: (a) first mode, (b) second mode, (c) third mode, and (d) fourth mode. Experimental variation: solid line and analytical variation: dashed line. $\Delta = 100(f_{und}-f_{dam})/f_{und}$.

configurations. The mode shapes are more or less the same in the two cases, hence these dynamic quantities do not provide, as it is known in Ref. [18], an adequate damage indicator, at least for the considered small damage levels represented by the depth of the notch.

In Table 3 there is a comparison between the experimental frequencies and their corresponding analytical estimates for both the undamaged and damaged arch. The analytical model overestimates the experimental frequencies and differences become higher as the mode order rises. For all examined cases the model turns out to be extremely accurate, with percentage errors below 4.0%.

Remark that the geometry is the *measured* one on the specimen and slightly differs from the nominal values reported in Table 1. The variation between the measured and the nominal dimensions of the cross-section does not exceed 0.15 mm.

Fig. 6 shows the relative variation of the natural frequencies between the damaged and the undamaged configurations as functions of the damage intensity. It is interesting to observe that the analytical model serves as a good representative of the experimental results, since the patterns of the two curves are similar for all the values of the damage severity.

In conclusion, Fig. 7 shows, for the undamaged arch, both the experimental and analytical values of the radial component of the displacement of the axis for the first four natural modes. It is apparent that there is a very good agreement between the two sets of values.

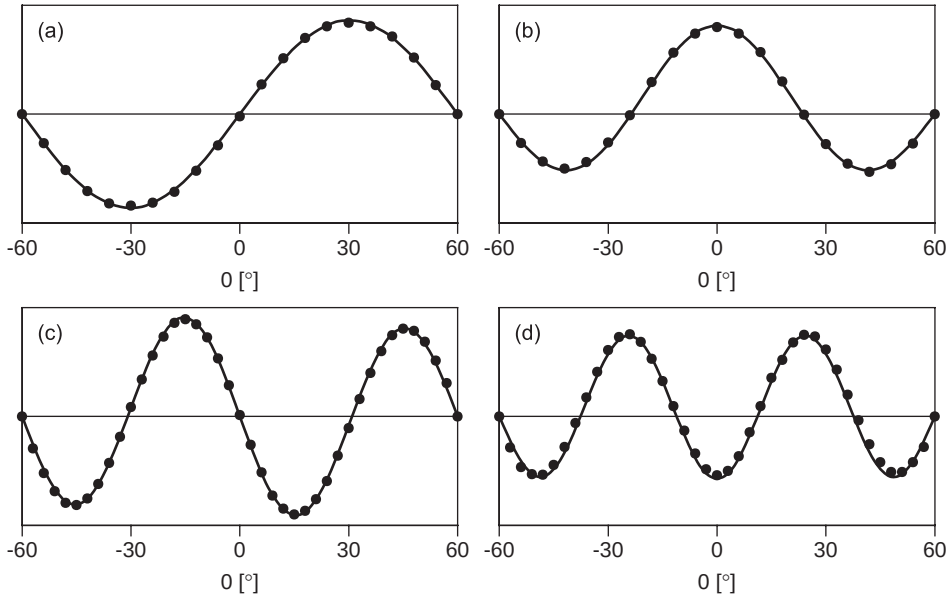

Fig. 7. First four experimental (dots) and analytical (solid line) modal shapes of the undamaged arch: (a) first mode, (b) second mode, (c) third mode, and (d) fourth mode.

3. Inverse problem

3.1. Frequency sensitivity to small damages

In this section, we try to determine the location and the amount of the damage intensity by means of an identification technique based on the measurements of the variation of the natural frequencies of the arch specimen between the undamaged and damaged configurations. In order to perform this procedure, we need to find an expression for the sensitivity of the natural frequencies induced by damage.

It would be possible to perform an analytical study of the arch in damaged configuration, in order to obtain the quantities of interest from the point of view of diagnostics for any amount of damage. Let us suppose, though, that the damage severity is "small", i.e., of order of magnitude $1/K$. It is reasonable to admit that the natural frequencies and the vibration modes in the undamaged and damaged configurations will not differ remarkably. It is then possible to extend the sensitivity analysis presented by Morassi [19] in the case of axial and bending vibration of rectilinear beams. Such analysis is based on a power expansion of the field equations in a neighbourhood of the undamaged configuration in terms of an arbitrary small parameter truncated at the first order. In this way, one can find that the ith axial frequency variation, for a given level of damage, is proportional to the square of the axial force in the ith undamaged mode shape evaluated at the damaged cross-section. Similarly, in the case of bending vibration the ith frequency variation is proportional to the square of the bending moment in the ith undamaged mode shape evaluated at the damaged cross-section.

If we suppose, as usual, the kinematical fields to be harmonic with respect to time, i.e.

$$u(\theta,t)=u(\theta)\cos(\omega t),\quad v(\theta,t)=v(\theta)\cos(\omega t),\quad \varphi(\theta,t)=\varphi(\theta)\cos(\omega t), \tag{6}$$

the field Eqs. (1) yield

$$\begin{aligned}
&\frac{EA}{R^2}\frac{\mathrm{d}}{\mathrm{d}\theta}\left(\frac{\mathrm{d}u(\theta)}{\mathrm{d}\theta}-v(\theta)\right)-\frac{GA}{R^2\chi}\left(u(\theta)+\frac{\mathrm{d}v(\theta)}{\mathrm{d}\theta}+R\varphi(\theta)\right)+\omega^2\rho A u(\theta)=0,\\
&\frac{GA}{R^2\chi}\frac{\mathrm{d}}{\mathrm{d}\theta}\left(u(\theta)+\frac{\mathrm{d}v(\theta)}{\mathrm{d}\theta}+R\varphi(\theta)\right)+\frac{EA}{R^2}\left(\frac{\mathrm{d}u(\theta)}{\mathrm{d}\theta}-v(\theta)\right)+\omega^2\rho A v(\theta)=0,\\
&\frac{EI}{R^2}\frac{\mathrm{d}^2\varphi(\theta)}{\mathrm{d}\theta^2}-\frac{GA}{R\chi}\left(u(\theta)+\frac{\mathrm{d}v(\theta)}{\mathrm{d}\theta}+R\varphi(\theta)\right)+\omega^2\rho I\varphi(\theta)=0.
\end{aligned} \tag{7}$$

The boundary and jump conditions for Eqs. (7) are formally identical to Eqs. (2) and (4), once it is understood that the dependence on time is dropped because of the positions (6). Let us pose

$$u(\theta) = u_0(\theta) + \varepsilon u_1(\theta), \quad v(\theta) = v_0(\theta) + \varepsilon v_1(\theta), \quad \varphi(\theta) = \varphi_0(\theta) + \varepsilon\varphi_1(\theta),$$
$$\lambda = \lambda_0 + \varepsilon\lambda_1, \quad \lambda = \omega^2, \tag{8}$$

where the subscript 0 refers to fields defined in the undamaged configuration, the subscript 1 stands for the first-order increment of the indicated field with respect to the undamaged configuration, and ε is a small perturbation parameter.

Let us substitute the positions (8) into Eqs. (7) and drop the terms of order higher than the first in ε. It is then possible to single out a group of addends defined in the undamaged configuration and hence identically satisfied. The remaining equations read as follows:

$$\frac{EA}{R^2}\frac{\mathrm{d}}{\mathrm{d}\theta}\left(\frac{\mathrm{d}u_1(\theta)}{\mathrm{d}\theta} - v_1(\theta)\right) - \frac{GA}{R^2\chi}\left(u_1(\theta) + \frac{\mathrm{d}v_1(\theta)}{\mathrm{d}\theta} + R\varphi_1(\theta)\right) + \rho\lambda_0 A u_1(\theta) + \rho\lambda_1 A u_0(\theta) = 0,$$
$$\frac{GA}{R^2\chi}\frac{\mathrm{d}}{\mathrm{d}\theta}\left(u_1(\theta) + \frac{\mathrm{d}v_1(\theta)}{\mathrm{d}\theta} + R\varphi_1(\theta)\right) + \frac{EA}{R^2}\left(\frac{\mathrm{d}u_1(\theta)}{\mathrm{d}\theta} - v_1(\theta)\right) + \rho\lambda_0 A v_1(\theta) + \rho\lambda_1 A v_0(\theta) = 0,$$
$$\frac{EI}{R^2}\frac{\mathrm{d}^2\varphi_1(\theta)}{\mathrm{d}\theta^2} - \frac{GA}{R\chi}\left(u_1(\theta) + \frac{\mathrm{d}v_1(\theta)}{\mathrm{d}\theta} + R\varphi_1(\theta)\right) + \rho\lambda_0 I\varphi_1(\theta) + \rho\lambda_1 I\varphi_0(\theta) = 0. \tag{9}$$

The positions (8) must be inserted in the boundary and jump conditions (2) and (4) as well. The zeroth order terms turn out to be trivial and have a typographical expression similar to the finite ones (2) and (4); they will not be reported for sake of brevity. The same considerations also hold for the boundary and jump conditions pertaining to the first-order set of Eqs. (9), with the exception of the jump condition on the rotation of the damaged cross-section, which reads

$$\varepsilon K(\varphi_1^{(2)}(\theta^D) - \varphi_1^{(1)}(\theta^D)) = \frac{EI}{R}\frac{\mathrm{d}\varphi_0(\theta^D)}{\mathrm{d}\theta}. \tag{10}$$

Let us multiply Eq. (9-1) by u_0, Eq. (9-2) by v_0, and Eq. (9-3) by φ_0, integrate the obtained expressions in the domain $[-\Theta,\Theta]$ and sum. Integrating by parts and suitably keeping into account the boundary and jump conditions both at the zeroth and the first order, we obtain an expression, which, introducing the normalisation condition

$$\int_{-\Theta}^{\Theta} \rho R(A(u_0^2 + v_0^2) + I\varphi_0^2)\,\mathrm{d}\theta = 1, \tag{11}$$

reads

$$\Delta\lambda \equiv \varepsilon\lambda_1 = -\frac{1}{K}(M_0(\theta^D))^2 = -\frac{1}{K}\left(EI\,\frac{\mathrm{d}\varphi_0(\theta^D)}{\mathrm{d}\theta}\right)^2. \tag{12}$$

As expected, expression (12) shows that the variation of frequency induced by a localised crack is determined as a ratio between the squared bending moment of the undamaged arch evaluated at the damaged cross-section θ^D and the severity K.

3.2. An application

Since we know from experimental data the variations of the natural frequencies, we are able to use Eq. (12) in order to detect the damage. Let us denote by $\Delta\lambda_j$ the variation associated with the jth natural mode; it is then possible to re-write Eq. (12) putting into evidence the damage severity as a function of the damage location:

$$K_j(\theta^D) = -\frac{(M_{0j}(\theta^D))^2}{\Delta\lambda_j}. \tag{13}$$

It is then possible to plot the curve $K_j(\theta^D)$ for each j; the intersection of two such curves for distinct modes will let us calculate both θ^D and K^j. Due to the geometrical symmetry of the problem, there are always two damage location candidates, symmetrically placed with respect to the mid-span of the arch. As it is pointed out also in a previous paper [6], two distinct modes are not sufficient to uniquely determine the damage location in one-half of the arch. On the other hand, by considering more than two curves, it is possible to reject non-meaningful damage location candidates. Since it is impossible to get rid of model and experimental errors, and because of the linearisation procedure adopted, the intersection of more than two curves is not a single point but rather a small neighbourhood of the actual solution.

It is then necessary to define a distance function

$$r(\theta^D) = \sum_{j \neq i} \left| K_j(\theta^D) - K_i(\theta^D) \right|. \tag{14}$$

In order to find the solution $\overline{\theta}^D$ of the inverse problem, we take the minimum of the distance function (14); then, we assume the damage severity $\overline{K}(\overline{\theta}^D)$ as a mean value

$$\overline{K}(\overline{\theta}^D) = \frac{1}{n} \sum_{j=1}^{n} K_j(\overline{\theta}^D), \tag{15}$$

n being the number of modes used in the identification procedure.

With the aim of testing the validity of the proposed technique, an identification application based on the experimental data obtained for the above-described arch specimen is performed. It is worth remarking that, since the proposed technique is based on the measurements of frequency variations, possible errors in the arch model do not meaningfully affect the obtained results, as it was previously remarked in Ref. [6]: indeed, in that paper a simple Euler–Bernoulli curvilinear beam is adopted and the error between the analytical and the pseudo-experimental data is remarkable, yet the identification procedure provides good results.

In Fig. 8 the plots of the distance function (14) are reported for all the amounts of damage considered and for different choices of the number of modes used in the identification technique. It is evident that in all the considered cases the loci of the minima are clearly well defined and the results are summarised in Table 4. The damage location in all cases is satisfactorily provided, with a relative error less than 2%. The number of modes used in the technique does not meaningfully influence the accuracy of the results. Indeed, on the one hand the

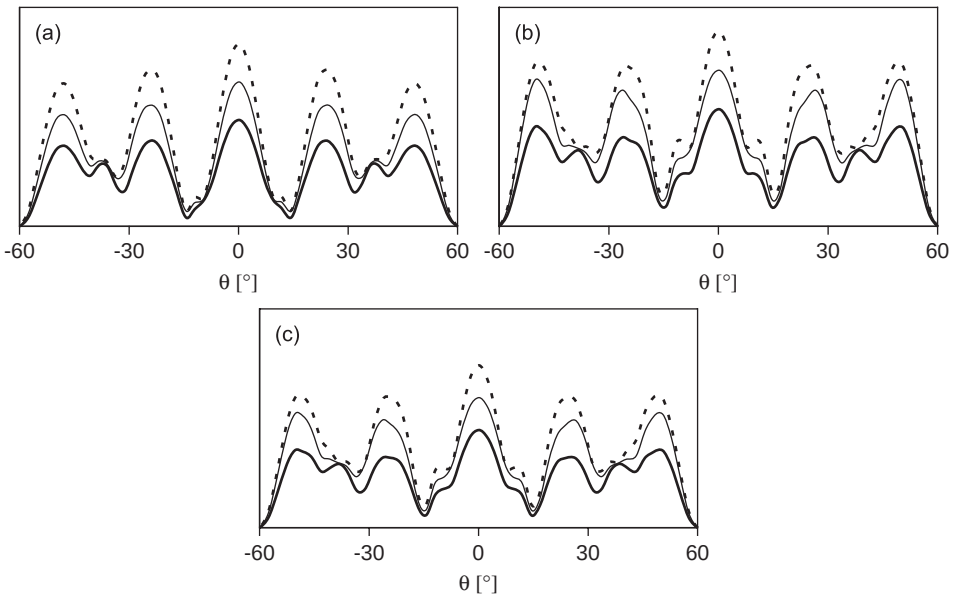

Fig. 8. Plots of the $r(\theta^D)$ functions for different damage intensities and number of modes used in the identification procedure: (a) damage D1, (b) damage D2, and (c) damage D3. $n = 3$, solid thick line; $n = 4$, solid thin line; and $n = 5$, dashed line.

Table 4
Identification of the damage location for different damage intensities and number of modes used

	Damage D1		Damage D2		Damage D3	
	θ^D (deg)	θ^D (deg)	θ^D (deg)	θ^D (deg)	θ^D (deg)	θ^D (deg)
$n=3$	−13.81	13.81	−14.60	14.60	−14.84	14.84
$n=4$	−14.42	14.42	−14.63	14.63	−14.64	14.64
$n=5$	−14.54	14.54	−15.75	15.75	−14.88	14.88
Actual location	16.50		16.50		16.50	

Table 5
Identification of the damage severity for different damage intensities and number of modes used

	Damage D1 K (kN m)	Damage D2 K (kN m)	Damage D3 K (kN m)
$n=3$	372.66	136.40	82.49
$n=4$	337.00	132.29	82.89
$n=5$	328.74	175.77	105.00
Cerri and Ruta [6]	1410.62	217.31	49.62
Ostachowicz and Krawczuk [20]	488.10	115.70	43.71

increasing number of modes lets us better identify the neighbourhood of the damage location; on the other hand, the analytical model is less accurate for higher-order modes, as it is already remarked in the previous section.

In Table 5 the results for the average damage intensity are shown and compared with others, one of which is obtained in function of the depth of the notch [20] and the other is based on the expression (3). The values are remarkably different, as expected: indeed, the damage is in any case modelled in a rather coarse way. On the other hand, it is apparent that the assessment of the damage intensity increases for all n with the depth of the notch, thus providing a reliable tool.

4. Conclusions

In this paper, the results of dynamical experimental tests performed on a circular steel arch are presented. The arch is tested in the undamaged configuration and in three different damaged configurations. The damage is obtained by operating a very narrow notch, which so could be thought of as affecting a single cross-section of the arch. Three damaged configurations are studied by considering increasing depths of the notch. The damage is modelled by supposing the two regular parts of the arch as being connected by a rotation spring of given stiffness, which so constitutes a measure of the damage severity. The arch is described as a 1D curvilinear beam according to the Timoshenko theory, and rotational inertia is also taken into account. The diagnostic, inverse problem is solved by means of an identification technique based on the measurements of the variations of natural frequencies between the undamaged and the damaged configurations. The sensitivity to damage is investigated by means of a formal series expansion in a neighbourhood of the undamaged configuration. The following conclusions can be drawn from the comparison between experimental and analytical data: (a) the experimental natural frequencies and vibration modes are well represented by the analytical model, at least for the first five modes; (b) the variation of the first five natural frequencies are clearly detectable and may be easily compared with the analytical data; (c) on the contrary, the radial components of the first four vibration modes turn out to be practically unaffected by the damage, hence cannot be assumed as a meaningful diagnostic tool, at least for the small damage amounts taken into consideration; (d) the identification yields very reliable results as far as the damage location is concerned, while it is only roughly accurate in evaluating the damage severity, always bearing in mind that the considered

damage is small. Further possible developments could involve the introduction of a more refined model of the damage and of the measure of the damage severity.

Acknowledgements

M. Dilena acknowledges the hospitality of the Dipartimento di Ingegneria Strutturale e Geotecnica of the University of Rome "La Sapienza" during his visit in April 2006. G.C. Ruta acknowledges the support of the grant "Progetto Giovani Ricercatori" of the University of Rome "La Sapienza" for the year 2002. The authors wish to thank Professor Antonino Morassi and Professor Fabrizio Vestroni for careful reading and their valuable help and suggestions.

References

[1] O.S. Salawu, Detection of structural damage through changes in frequencies: a review, *Engineering Structures* 19 (1997) 718–723.
[2] S.W. Doebling, C.R. Farrar, M.B. Prime, A summary review of vibration-based damage identification methods, *Shock and Vibration Digest* 30 (1998) 91–105.
[3] D. Capecchi, F. Vestroni, Monitoring of structural systems by using frequency data, *Earthquake Engineering and Structural Dynamics* 28 (1999) 447–461.
[4] F. Vestroni, D. Capecchi, Damage detection in beam structures based on frequency measurements, *ASCE Journal of Engineering Mechanics* 126 (2000) 761–768.
[5] A. Morassi, Identification of a crack in a rod based on changes in a pair of natural frequencies, *Journal of Sound and Vibration* 242 (2001) 577–596.
[6] M.N. Cerri, G.C. Ruta, Detection of localised damage in plane circular arches by frequency data, *Journal of Sound and Vibration* 270 (2004) 39–59.
[7] M.N. Cerri, F. Vestroni, Identification of damage due to open cracks by changes of measured frequencies, *Proceedings of the XVIth AIMETA Congress*, Ferrara, Italy, 2003 (full text in CD-Rom).
[8] J. Henrych, *Dynamics of Arches and Frames*, Elsevier, Amsterdam, 1981.
[9] A.E.H. Love, *A Treatise on the Mathematical Theory of Elasticity*, Dover, New York, 1944.
[10] A.S. Veletsos, M.J. Austin, C.A. Lopes Pereira, S.-J. Wung, Free vibration of circular arches, *ASCE Journal of Engineering Mechanics* 98 (1972) 311–329.
[11] N.M. Auciello, M.A. De Rosa, Free vibrations of circular arches: a review, *Journal of Sound and Vibration* 176 (1994) 433–458.
[12] E. Tüfekçi, A. Arpaci, Exact solution of in-plane vibrations of circular arches with account taken of axial extension, transverse shear and rotatory inertia, *Journal of Sound and Vibration* 209 (1998) 845–856.
[13] E. Viola, E. Artioli, M. Dilena, Analytical and G.D.Q. results for vibration analysis of damaged circular arches, *Journal of Sound and Vibration* 288 (2005) 887–906.
[14] E. Viola, M. Dilena, F. Tornabene, Analytical and numerical results for vibration analysis of multi-stepped and multi-damaged circular arches, *Journal of Sound and Vibration* 299 (1–2) (2007) 143–163.
[15] M.N. Cerri, F. Vestroni, Detection of damage in beams subjected to diffused cracking, *Journal of Sound and Vibration* 234 (2000) 259–276.
[16] M. Krawczuk, W.M. Ostachowicz, Natural vibrations of a clamped–clamped arch with an open transverse crack, *Journal of Sound and Acoustics* 119 (1997) 145–151.
[17] D.J. Ewins, *Modal Testing: Theory, Practice and Application*, Research Studies Press Ltd., Baldock, 1981.
[18] A.K. Pandey, M. Biswas, M.M. Samman, Damage detection from changes in curvature mode shapes, *Journal of Sound and Vibration* 145 (1991) 321–332.
[19] A. Morassi, Crack-induced changes in eigenparameters of beam structures, *ASCE Journal of Engineering Mechanics* 119 (1993) 1798–1803.
[20] W.M. Ostachowicz, M. Krawczuk, Analysis of the effect of a crack on the natural frequencies of a cantilever beam, *Journal of Sound and Vibration* 150 (1991) 191–201.